

EFFECT OF ENERGY DISSIPATION RATE ON THE MICROMIXING IN A MICROREACTOR WITH FREE IMPINGING JETS

A.A. Sirotkin¹, R.Sh. Abiev^{1,2*}

¹St. Petersburg State Technological Institute (Technical University), Saint-Petersburg, Russia

²Grebenshchikov Institute of Silicate Chemistry, Russian Academy of Sciences,
Saint-Petersburg, Russia

Abstract. An experimental study of micromixing processes in a liquid sheet formed in a microreactor with impinging jets has been carried out. An apparatus with differential sampling was used. To determine the quality of micromixing, the segregation index, determined by the iodide-iodate method, was defined. It is shown that there are two regions according to the flow rates of supplied solutions in jets. In the first region, with an increase in flow rate Q_j (and energy dissipation rate ε), the segregation index X_s decreases, and in the second region, X_s slowly increases. This behavior is explained due to the fact that after reaching the critical value of the flow rate, an accelerated disintegration of the liquid sheet begins, leading to a deterioration in the quality of micromixing. Thus, the first area recommended for practice with $X_s \approx 0.001-0.002$ (note that for reactor with magnetic stirrer $X_s = 0.5$) is the one in which a stable liquid sheet is formed, and the dependence $X_s = f(\varepsilon_i)$ has the form $X_s = 0.206 \varepsilon_i^{-0.335}$. The exponent in this relation (-0.335) is similar to that obtained in Falk & Commengen (2010) (-0.45) for the micromixing time: $t_m = 0.15 \varepsilon^{-0.45}$.

Keywords: microreactor, micromixing, energy dissipation rate, impinging jets.

Corresponding Author: Rufat Abiev, St. Petersburg State Technological Institute (Technical University), Saint - Petersburg, Russia, Tel.: +7 981 131 22 78, e-mail: abiev.rufat@gmail.com

Received: 22 June 2022;

Accepted: 15 August 2022;

Published: 7 December 2022.

1. Introduction

Microreactor with free impinging jets (MRFIJ) is a kind of microreactors, the distinguishing feature of which is the value of the transverse size of the apparatus (the diameter of the jets), which is in the range from about 0.1 mm to 2-3 mm.

Microreactors with free impinging jets are increasingly used in the synthesis of nanosized particles of inorganic materials. Synthesis of nanosized particles takes place either directly in the microreactor itself (at room temperature and atmospheric pressure), as, for example, during the formation of CoFe₂O₄ (Abiev *et al.*, 2017), LaPO₄ (Proskurina *et al.*, 2019a), or with subsequent heat treatment, for example, in synthesis of BiFeO₃ (Proskurina *et al.*, 2021; 2019b), GdFeO₃ (Albadri *et al.*, 2020; 2021a; 2021b).

Microreactors with free impinging jets have been known since at least from the 1950s, when they were used by NASA to form fine droplets of propellant in the combustion chamber of liquid propellant rocket engines (Heidmann & Humphrey,

How to cite (APA):

Sirotkin, A.A., Abiev, R.Sh. (2022). Effect of energy dissipation rate on the micromixing in a microreactor with free impinging jets. *New Materials, Compounds and Applications*, 6(3), 191-201.

1951; Ashgriz *et al.*, 2001), i.e. initially, MRFIJ was considered as a tool for the formation of droplets (“atomization”) (Ryan *et al.*, 1995; Handbook of Atomization & Sprays, 2011). It should be noted that in this case freely colliding jets were considered. Already in the 1990s, the first attempts were made to use this principle to carry out fast reactions, mainly precipitation reactions, there were microreactors with free colliding jets created.

The MRFIJ schematic is shown in Fig. 1. In MRFIJ, jets of solutions 1, having a diameter of about 0.5–2 mm (Fig. 1), are fed at fairly high and equal velocities (as a rule, up to 10–16 m/s) in a vertical plane at an angle of 2θ (which can be in the range from 60° to 180°). When they collide, a liquid sheet 3 is formed, with some thickening in the collision zone 3. In the sheet 3 intensive micromixing occurs, characterized by extremely high values of the specific energy dissipation rate (in the order of 10^4 - 10^6 W/kg) (Proskurina *et al.* 2018; Abiev, 2020a;b; 2021a; 2022a), which is both due to the small volume of the mixing zone (no more than 0.5 mL) and high kinetic energy of the jets. Nucleation and primary growth of particles take place in the liquid sheet. The suspension 4 formed during the contact of solutions (for example, a mixture of salt solutions and an antisolvent solution) is collected in a flask. If it is necessary to prevent further growth of particles, appropriate measures should be taken: the resulting suspension is to be frozen, subjected to rapid washing, etc.

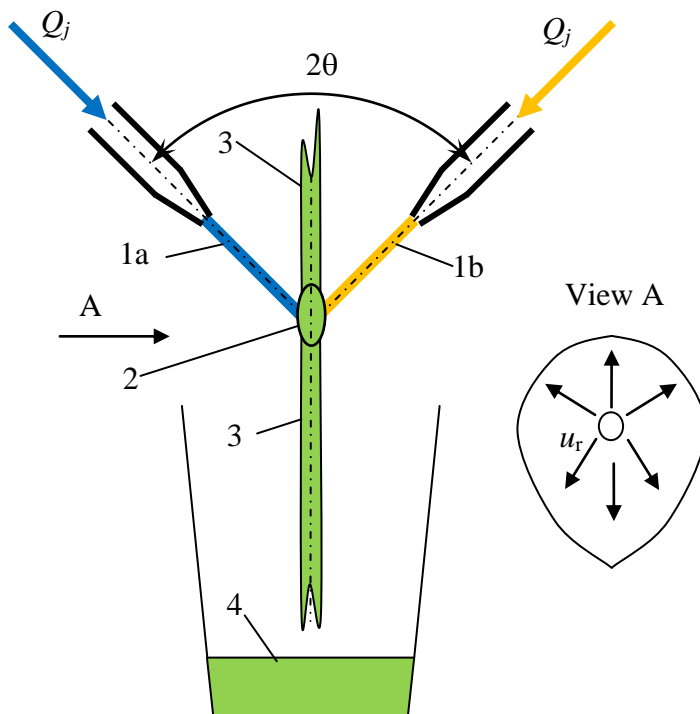


Fig. 1. A general schematic diagram of microreactor with free impinging jets: 1 – jets of solutions of reagents and antisolvent; 2 – jet collision zone; 3 – liquid sheet; 4 – suspension with nanosized particles. u_r is a radial velocity in the sheet, Q_j – flow rate in jets.

Falk and Commenge (2010) compared eight types of microreactors with high micromixing quality. It is shown that the microchannel diameter in the range from 50 μm to 1 mm has practically no effect on the mixing time t_m , while the specific energy

dissipation rate has a decisive effect, the general dependence for all studied microreactors has the form $t_m = 0.15 \varepsilon^{-0.45}$.

One of the key problems in the design of MRFIJ is to identify the optimal operating conditions, as well as to determine the following dependencies: the specific energy dissipation rate on the jet flow rate, the segregation index on the jet flow rate, and the segregation index on the specific energy dissipation rate.

The purpose of this work is to determine these dependencies. On the basis of such dependences, an engineering method for calculating microreactors with colliding jets has been developed.

2. Experimental part

For the study of hydrodynamics, a high-speed photography (semi-professional camera Canon D40, with a specialized macro lens Canon EF-S macro 60/f 2.8 and a professional flash Canon EX 580, shooting was carried out with an exposure time of $1.25 \cdot 10^{-4}$ s) was used.

As a tool for studying the quality of micromixing, the iodide-iodate method (Guichardon & Falk, 2000; Guichardon *et al.*, 2000; Falk & Commenge, 2010; Kölbl *et al.*, 2008; 2010; Commenge & Falk, 2011; Jasinska, 2015) was chosen.

At the Department of Optimization of Chemical and Biotechnological Equipment of St. Petersburg State Institute of Technology (TU), in order to study the processes occurring in this technological system, a laboratory facility was developed based on a microreactor with free impinging jets, which included several modifications of MRFIJ: 1) for the synthesis of oxide materials and micromixing study - with a solid glass body (Proskurina *et al.*, 2021); 2) to study the geometry and conditions for the formation and disintegration of a liquid sheet – an open-frame MRFIJ, in which the nozzles were fixed at a given angle 2θ on a PVC frame and installed inside a rectangular glass container (Abiev & Sirotkin, 2022). Part of the experiments to determine the parameters of micromixing using the iodide-iodate technique was carried out using differential sampling of reaction products: directly under the jet collision zone and at the periphery (Abiev & Sirotkin, 2020) (Fig. 2).

The solutions were supplied by two gear pumps TOPSFLO Micro Pump Technology (model MG213XKDC24WI) with a nominal flow rate of up to 3500 mL/min and an operating pressure of up to 10 bar. The material of the inner part of the housing is AISI 316L stainless steel, the gears are PEEK, the seals are PTFE.

To determine the volumetric flow rates of solutions, two VISION® 1005 2F66 turbine flowmeters with a bore diameter of 5 mm, flow measurement limits of 100–2500 mL/min with a relative measurement error of $\pm 3\%$, equipped with electronic digital indicating units ILR750T 56704, were used. The flowmeters were connected to an analog digital converter L-Card-14-140 and a laptop with PowerGraph software necessary for collecting, recording and processing measured data.

In this study, MRFIJ was used (see Fig. 2) with the following parameters: glass nozzles with a diameter of $d_j = 1$ mm with an angle between them $2\theta = 90^\circ$, the distance between the nozzle outlet and the collision point $L = 17$ mm, the distance between the nozzles $B = 25$ mm. Nozzles are located in a vertical plane.

As the jet velocity increases, the sheet sizes first increase, and then at certain flow rate (for the studied case, starting from 400 mL/min), the sheet disintegrates (Abiev & Sirotkin 2020).

To conduct studies to determine the quality of micromixing using the iodite-iodate technique, the recommendations given in (Guichardon & Falk, 2000) were used. In this work, sets of concentrations are given (Table 1) corresponding to the optimal optical densities that can be measured by means of UV-VIS spectrophotometer.

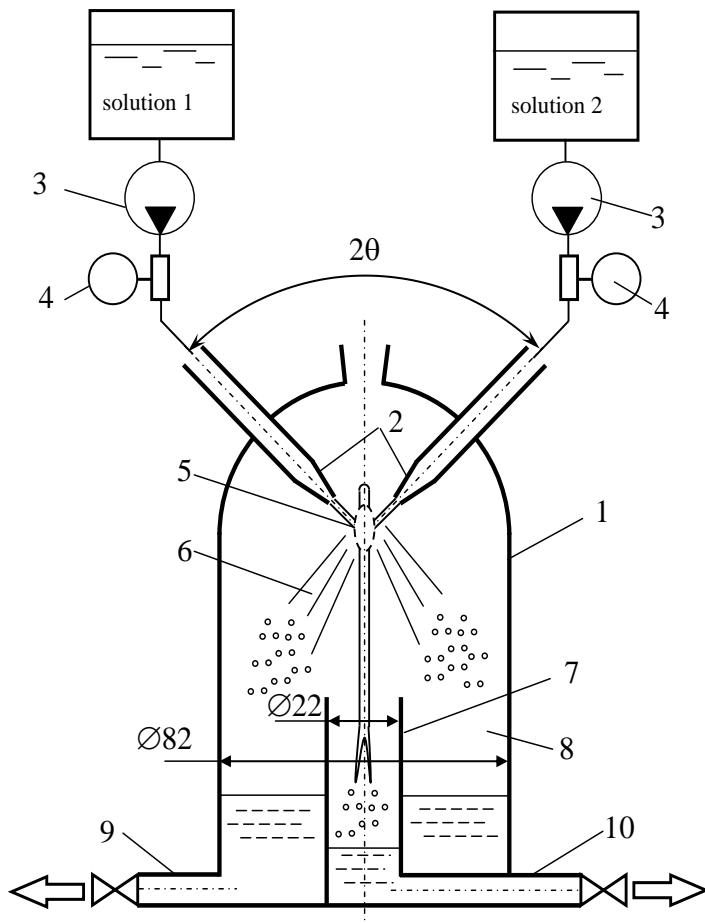


Fig. 2. Laboratory setup for studying micromixing with differential sampling of reaction products: directly under the jet collision zone and on the periphery: 1 – MRFIJ housing; 2 - nozzles; 3 - gear pumps; 4 – flowmeters; 5 – jet collision zone; 6 - zone of splashes expansion to the walls of the reactor; 7 – beaker for liquid collecting from the central zone; 8 – an annular zone for collecting liquid from splashes; 9, 10 - nipples for the removal of reaction products

Table 1. Recommended combinations of reagent concentrations for the experimental determination of the micromixing quality in microreactors (Guichardon & Falk, 2000; Falk & Commengé, 2010)

Concentration, mol/L	Reagent concentration combination number					
	1	1b	1c	2	2b	2c
[H ⁺]	0.03	0.06	0.04	0.015	0.03	0.02
[KI]	0.032	0.032	0.032	0.016	0.016	0.016
[KIO ₃]	0.006	0.006	0.006	0.003	0.003	0.003
[NaOH]	0.09	0.09	0.09	0.045	0.045	0.045
[H ₃ BO ₃]	0.09	0.09	0.09	0.045	0.045	0.045

As a result of preliminary studies, an optimal set of concentrations was selected (combination 2 in Table 1), which was used in all experiments.

The scheme of differentiated sampling in MRSS is shown in Fig. 2. Part of the obtained product was collected in a beaker 7 with an inner diameter of 22 mm (central product collection zone), the rest of the product was collected in a peripheral annular zone 8 formed by a body with a diameter of 82 mm and a beaker 7. The mass of the obtained samples was weighed with an accuracy of 0.1 g, then optical density of the samples was measured by means of SF-2000 spectrophotometer at a wavelength of $\lambda = 353$ nm for five samples filled into 10 mm thick quartz cuvettes.

Fig. 3 shows the characteristic shape of the liquid sheet and its main dimensions, the jet collision zone with specific energy dissipation rate ε_i , and the energy dissipation zone in the liquid sheet ε_e (Abiev & Sirotkin, 2022).

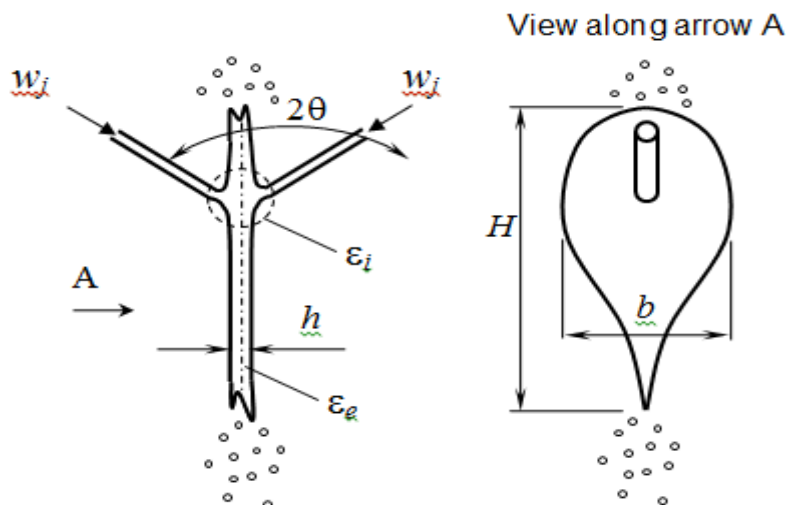


Fig. 3. Schematic of formation process and main dimensions of the liquid sheet in the MRFIJ: 2θ – angle between the jets; H – height of the sheet; b – width of the sheet; h – thickness of the liquid sheet

3. Results and discussion

Mass fraction of samples φ was determined for each experiment as follows:

$$\varphi = (\text{sample mass in the center}) / (\text{total sample mass}).$$

Fig. 4 illustrates the distribution of fluid mass between center and periphery. At $Q_j \leq 300$ mL/min, the value of φ decreases from 0.86 (at 100 mL/min) and 0.42 (at 300 mL/min), and at $Q_j \geq 700$ mL/min, the mass fraction of liquid collected in the center practically stabilizes at the level of 17.5-23.5% of the total weight of the product. Fig. 5 shows the dependences of the segregation index X_s for the central and peripheral zones, as well as the weighted average value of mean(X_s) on the jet flow rate Q_j .

In Abiev & Sirotkin (2022), the mechanism for separating a mixture into two parts is with high quality of micromixing (sample in the central zone for $Q_j \geq 700$ mL/min) and low quality of micromixing (sample in the peripheral zone for $Q_j \geq 700$ mL/min) is explained by the nonuniformity of the velocity profile: near the walls there is a near-wall laminar layer with a velocity on the wall $w_w = 0$, in the central part there is a flow

core with a maximum velocity on the jet axis. As soon as the jets leave the nozzles, they begin to rebuild the velocity profile, but because of the short distance between the nozzles (the distance from the nozzle exit to the collision plane was $L = 17$ mm), it does not have time to complete.

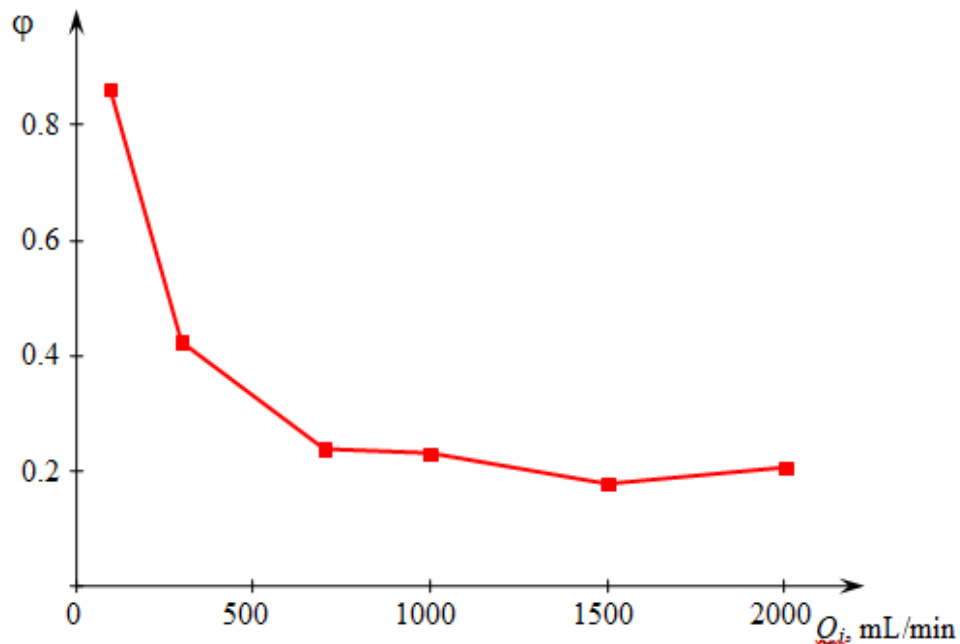


Fig. 4. Dependence of the mass fraction of samples φ on the jet flow rate Q_j (mL/min) in the MRFIJ (Abiev & Sirotnik, 2020)

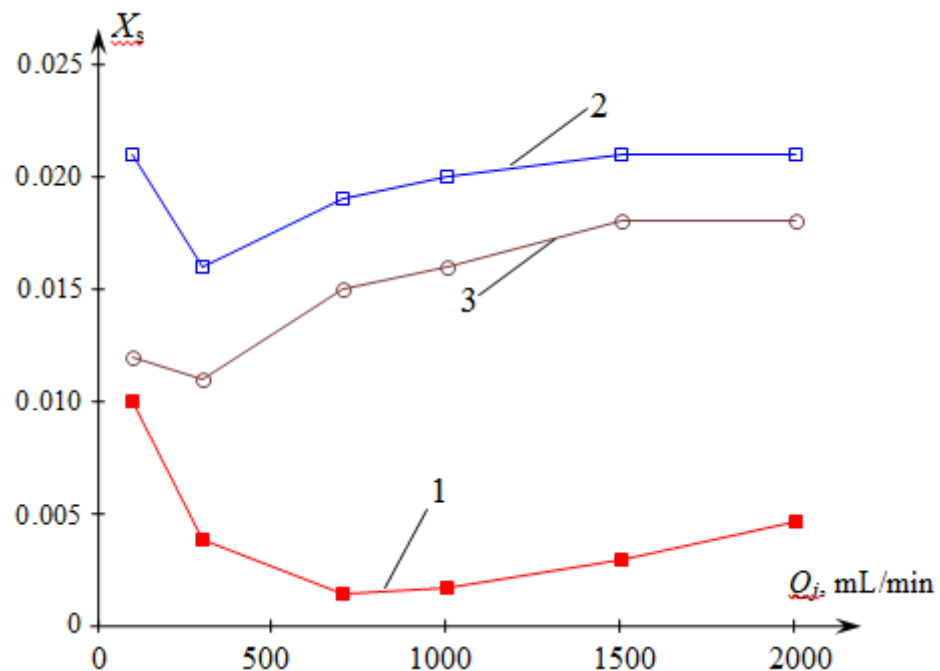


Fig. 5. Dependence of the segregation index X_s on the jet flow rate Q_j (mL/min) in the MRFIJ in the samples taken: 1 – in the center; 2 – on the periphery; 3 – weighted average (Abiev & Sirotnik, 2020)

As a result, before the collision of the jets in the cross section of the jets, it is possible to distinguish a central zone with a high velocity (zone of intense micromixing), and around it, an annular zone with a velocity close to zero (zone of passive micromixing). In the process of jet collision in the zone of collision of the cores of the flows (with a sufficiently accurate coincidence of the centers of the jets), the best micromixing occurs, because local speeds are maximum there; in the annular jet zone, micromixing is much worse, since the velocities in this zone are close to zero.

Thus, at high flow rates, the liquid from the annular zone of the jets, which is not well mixed, practically does not enter the central sampling zone, but scatters in the form of ligaments and drops and falls mainly into the peripheral sampling zone.

According to the mechanism described above, at low flow rates significant amount (e.g. 86% at $Q_j = 100 \text{ mL/min}$) of not perfectly mixed liquid is collected in the center and directly affects the measured quality of micromixing.

At higher flow rates ($Q_j \geq 700 \text{ mL/min}$), the mixture in the form of drops and ligaments, not subjected to intense micromixing, flies to the periphery, and therefore, almost only the product with a high quality of micromixing is collected in the central zone resulting in the better (lower) X_s values.

The optimum flow rate for the central sampling area is 700 mL/min (line 1 in Fig. 5). The average segregation index X_s (line 3 in Fig. 5) has a local minimum at $Q_j = 300 \text{ mL/min}$, and at higher flow rates it monotonically increases up to a flow rate of 1500 mL/min, after which it slightly decreases. Such a behavior of the curve $X_s = f(Q_j)$ (line 3 in Fig. 5) indicates that the optimal micromixing conditions are achieved on average for the sample at a flow rate of $Q_j = 300 \text{ mL/min}$. Comparison of lines 1 and 2 in Figs. 5 shows that from the point of view of achieving the highest quality, it is advisable to select the product from the central zone, where the best micromixing is achieved ($X_s \rightarrow \min$). Although from a practical point of view, such a process will lead to some decrease in the overall productivity of the apparatus and a decrease in yield, the quality of micromixing achieved by this may be a more important factor in choosing the operating mode of the reactor. Note that even the maximum value of the segregation index, obtained at a flow rate of 2000 mL/min, is $\max(X_s) = 4.7 \times 10^{-3}$, which is two orders of magnitude better than in the apparatus with a magnetic stirrer.

To obtain approximations $X_s = f(Q_j)$ for the central sampling zone (line 1 in Fig. 5), it seemed logical to distinguish two areas of flow rates with a threshold value $Q_j = 700 \text{ mL/min}$, above which the liquid sheet begins to disintegrate rapidly, with the general equation:

$$X_s = B Q_j^n \quad (1)$$

The values of the coefficients B and exponents n for these two areas, obtained as a result of processing the experimental data by the least squares method, are presented in Table 2. The positive sign of the exponent n reflects the fact that at $Q_j > 700 \text{ mL/min}$ there is some (insignificant) increase in the X_s value in the central sampling zone.

Table 2. Values of parameters B and n in equation (1) (flow rate Q_j is in mL/min)

Flow rates Q_j	$B, (\text{min/mL})^n$	n
$Q_j < 700 \text{ mL/min}$	1.098	-1.006
$Q_j > 700 \text{ mL/min}$	9.74×10^{-8}	1.416

Processing of the data presented in Table 3, allowed to get dependencies $\varepsilon_i = f(Q_j)$ and $\varepsilon_e = f(Q_j)$ in the following form

$$\varepsilon_i = A_i Q_j^{n_i} \quad (2)$$

$$\varepsilon_e = A_e + n_e Q_j. \quad (3)$$

Table 3. Values of parameters A_i , A_e , n_i , n_e in equations (2), (3) (flow rate Q_j is in mL/min) according to the data presented in Table 2

Flow rates Q_j	For the collision zone		For the liquid sheet	
	A_i , W/kg·(min/mL) ^{1/3}	n_i	A_e , W/kg	n_e , W·min/(kg·mL)
$Q_j = 100\text{--}2000$ mL/min	6.743×10^{-3}	3.0	-7.518	2.922

From equations (1)–(3), it is easy to obtain dependencies relating X_s to the specific energy dissipation rate:

- 1) Relation between X_s and ε_i :

$$X_s = B \left(\frac{\varepsilon_i}{A_i} \right)^{\frac{n}{n_i}} = C_i \varepsilon_i^{m_i}, \quad (4)$$

where $C_i = B \left(\frac{1}{A_i} \right)^{m_i}$, $m_i = n/n_i$.

- 2) Relation between X_s and ε_e :

$$X_s = B \left(\frac{\varepsilon_e - A_e}{n_e} \right)^n \quad (5)$$

The values of the parameters in equation (4) were calculated using data from Tables 2 and 3, and are presented in Table 4; the values of the parameters in equation (5) are already shown in Tables 2 and 3.

Table 4. Values of parameters C_i , m_i in equation (4) (flow rate Q_j is in mL/min)

Flow rates Q_j	For the collision zone	
	C_i , (kg/W) ^{mi}	m_i
$Q_j < 700$ mL/min	0.206	-0.335
$Q_j > 700$ mL/min	1.822×10^{-8}	0.472

It is worth to note that for the region of low flow rates ($Q_j < 700$ mL/min), when a stable liquid sheet is formed, the dependence $X_s = f(\varepsilon_i)$ having the form of equation (6)

$$X_s = 0.206 \varepsilon_i^{-0.335} \quad (6)$$

has an exponent $m_i = -0.335$ having a value close to the same exponent (-0.45) in the ratio for the micromixing time obtained in Falk & Commenge (2010) ($t_m = 0.15 \varepsilon^{-0.45}$), thus indicating a correlation between the micromixing time t_m studied earlier and the segregation index X_s studied in this work.

The positive value of the exponent for the region of high flow rates ($Q_j > 700$ mL/min) $m_i = 0.472$ demonstrates, on the one hand, the deterioration of the quality of micromixing with an increase in ε_i due to the disintegration of the liquid sheet, on the other hand, the growth of the segregation index in this case not as significant as could be seen from the plot in Fig. 5.

5. Conclusion

It is shown that there is an optimal fluid flow rate in the jets, above which the liquid sheet disintegrates. For the studied parameters, it is 700 mL/min, which corresponds to the jet Weber number $We_j = 3065$.

The parameters of the dependence (1) $X_s = f(Q_j)$ are obtained, which relate the micromixing quality characteristic (segregation index X_s) with the jet flow rate Q_j , as well as the specific energy dissipation rate with the liquid flow rate in the jet: equation (2) for the jet collision zone $\varepsilon_i = f(Q_j)$ and equation (3) for the volume of the entire liquid sheet $\varepsilon_e = f(Q_j)$.

In addition, equations (4) and (5) were obtained that relate the segregation index X_s to the specific energy dissipation rate ε_i and ε_e , respectively.

On the basis of the obtained equations and recommendations, an algorithm for calculating the MRFIJ parameters is developed, which is shown in Fig. 6. Some of the parameters are to be chosen or calculated using recommendations and equations provided in our previous works, and the eqs. (1)-(5) are elaborated in the presented paper.

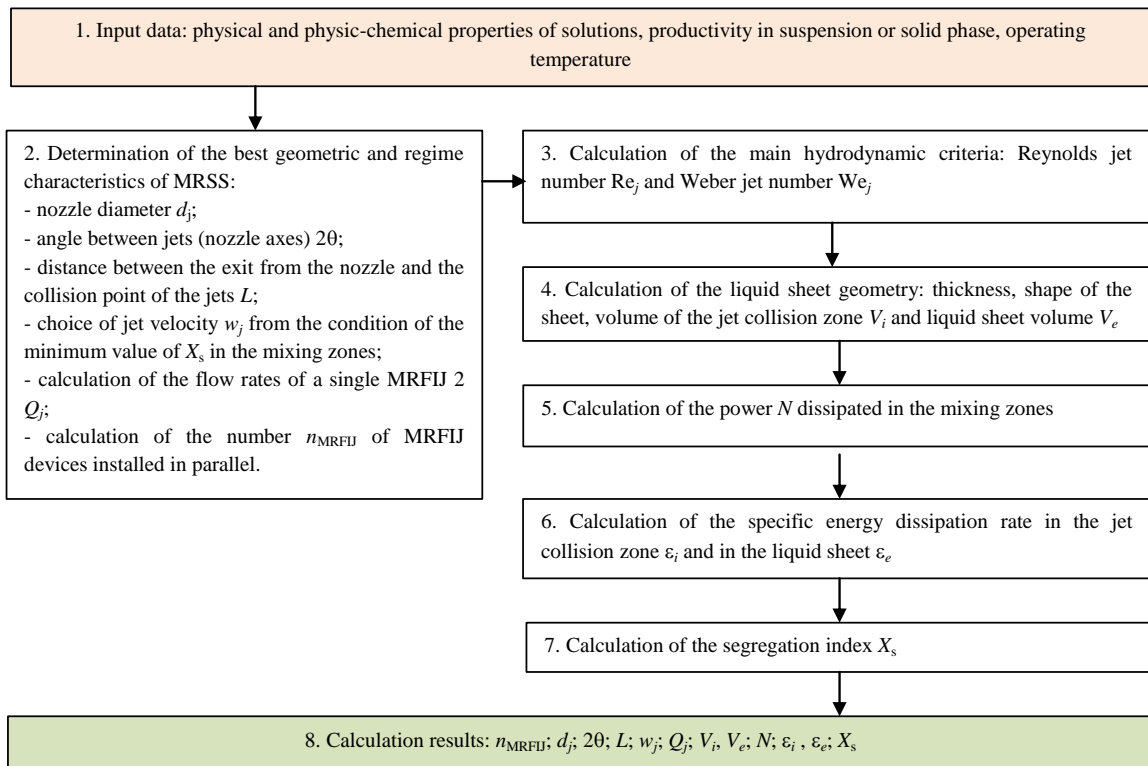


Fig. 6. Algorithm for calculating of MRFIJ parameters

Acknowledgments

The reported study was funded by RFBR, project number 19-33-90299.

References

- Abiev, R.S., Almyasheva, O.V., Izotova, S.G., & Gusarov, V.V. (2017). Synthesis of cobalt ferrite nanoparticles by means of confined impinging-jets reactors. *J. Chem. Tech. App.*, 1(1), 7-13.
- Abiev, R.Sh. (2020a). Miniaturization as One of the Paths to Process Intensification in Chemical Engineering. *Theor. Found. Chem. Eng.* 54, 1–2; doi: 10.1134/S0040579520300016
- Abiev, R.S. (2020b). Impinging-Jets Micromixers and Microreactors: State of Art and Prospects for Use in the Chemical Technology of Nanomaterials (Review). *Theor. Found. Chem. Eng.*, 54, 1131–1147; DOI: 10.1134/S0040579520060019
- Abiev, R.Sh., Proskurina, O.V., Enikeeva, M.O., & Gusarov, V.V. (2021a). Effect of Hydrodynamic Conditions in an Impinging-Jet Microreactor on the Formation of Nanoparticles Based on Complex Oxides. *Theor. Found. Chem. Eng.*, 55, 12–29; doi: 10.1134/S0040579521010012
- Abiev, R.S., Almjashsheva, O.V., Popkov, V.I., & Proskurina, O.V. (2022a). Microreactor synthesis of nanosized particles: The role of micromixing, aggregation, and separation processes in heterogeneous nucleation. *Chem. Eng. Res. & Des.*, 178, 73-94; doi: 10.1016/j.cherd.2021.12.003
- Abiev, R.S., Sirotkin, A.A. (2020). Influence of hydrodynamic conditions on micromixing in microreactors with free impinging jets. *Fluids*, 5(4), 179.
- Abiev, R.Sh., Sirotkin A.A. (2022). Effect of Hydrodynamic Conditions on Micromixing in Impinging-Jets Microreactors. *Theor. Found. Chem. Eng.*, 56(1), 9–22. doi: 10.1134/S0040579522010018
- Albadi, Y., Sirotkin, A.A., Semenov, V.G., Abiev, R.S., & Popkov, V.I. (2020). Synthesis of superparamagnetic GdFeO₃ nanoparticles using a free impinging-jets microreactor. *Russian Chemical Bulletin (Int. Ed.)*, 69(7), 1290-1295. doi: 10.1007/s11172-020-2900-x
- Albadi, Y., Ivanova, M.S., Grunin, L.Y., Martinson, K.D., Chebanenko, M.I., Izotova, S.G., ... & Popkov, V.I. (2021a). The influence of co-precipitation technique on the structure, morphology and dual-modal proton relaxivity of GdFeO₃ nanoparticles. *Inorganics*, 9(5), 39.
- Abiev, R.S., Almjashsheva, O.V., Popkov, V.I., & Proskurina, O. . (2022). Microreactor synthesis of nanosized particles: The role of micromixing, aggregation, and separation processes in heterogeneous nucleation. *Chemical Engineering Research and Design*, 178, 73-94.
- Ashgriz, N., Brocklehurst, W., & Talley D. (2001). Mixing Mechanisms in a Pair of Impinging Jets. *J. Propul. Power.*, 17(3), 736-749. doi 10.2514/2.5803
- Commengé, J.-M., & Falk, L. (2011). Villermaux–Dushman protocol for experimental characterization of micromixers. *Chem. Eng. & Proc.*, 50, 979–990.
- Falk, L., Commengé, J.-M. (2010). Performance comparison of micromixers. *Chem. Eng. Sci.*, 65, 405-411. DOI: 10.1016/j.ces.2009.05.045
- Guichardon, P., Falk L. (2000). Characterisation of micromixing efficiency by the iodide-iodate reaction system. Part I: Experimental procedure. *Chem. Eng. Sci.*, 55, 4233–4243. doi: 10.1016/S0009-2509(00)00068-3
- Guichardon, P., Falk, P., & Villermaux, J. (2000). Characterisation of mixing efficiency by the iodide/iodate reaction system. Part 2. Kinetic study. *Chem. Eng. Sci.*, 55, 4243–4245. doi: 10.1016/S0009-2509(00)00069-5
- Heidmann, M.F., Humphrey J.C. (1951). Fluctuations in a Spray Formed by Two Impinging Jets. *NASA TN 2349*, April 1951.

- Handbook of Atomization and Sprays (2011). Ed. N. Ashgriz. Toronto: Springer Science + Business Media, LLC, Ch. 30, 685-707. doi 10.1007/978-1-4419-7264-4_30
- Jasińska, M. (2015). Test reactions to study efficiency of mixing. *Chem. Process Eng.*, 36(2), 171-208.
- Kölbl, A., Kraut, M., & Schubert, K. (2008). The iodide-iodate method to characterize microstructured mixing devices. *AIChE J.*, 54, 639–645. doi: 10.1002/aic.11408
- Kölbl, A., Schmidt-Lehr S. (2010). The iodide-iodate reaction method: The choice of the acid. *Chem. Eng. Sci.*, 65, 1897-1901. doi: 10.1016/j.ces.2009.11.032
- Proskurina, O.V., Nogovitsin, I.V., Il'ina, T.S., Danilovich, D.P., Abiev, R.Sh., & Gusarov, V.V. (2018), Formation of BiFeO₃ Nanoparticles Using Impinging Jets Microreactor. *Russ J. Gen. Chem.*, 88(10), 2139–2143
- Proskurina, O.V., Sivtsov, E.V., Enikeeva, M. O., Sirotkin, A.A., Abiev, R. Sh., & Gusarov, V.V. (2019a). Formation of rhabdophane-structured lanthanum orthophosphate nanoparticles in an impinging jets microreactor and rheological properties of sols based on them. *Nanosystems: Physics, Chemistry, Mathematics*, 10(2), 206–214. doi: 10.17586/222080542019102206214
- Proskurina, O.V., Abiev, R.S., Danilovich, D.P., Panchuk, V.V., Semenov V.G., Nevedomsky, V.N., & Gusarov, V.V. (2019b). Formation of nanocrystalline BiFeO₃ during heat treatment of hydroxides co-precipitated in an impinging-jets microreactor. *Chem. Eng. & Proc.: Proc. Intens.*, 143, 107598. doi: 10.1016/j.cep.2019.107598
- Proskurina, O.V., Sokolova, A.N., Sirotkin, A.A., Abiev, R.Sh., & Gusarov, V.V. (2021). Role of Hydroxide Precipitation Conditions in the Formation of Nanocrystalline BiFeO₃. *Russ. J. Inorg. Chem.*, 66(2), 163–169. doi: 10.1134/S0036023621020157
- Ryan, H.M., Anderson, W.E., Pal S., & Santoro, R.J. (1995). Atomization Characteristics of Impinging Liquid Jets. *J. Prop. & Power*, 11(1), 135–145.